Time-Variant Channel Estimation Using Discrete Prolate Spheroidal Sequences

Thomas Zemen, *Member, IEEE,* and Christoph F. Mecklenbräuker, *Member, IEEE*

Abstract—We propose and analyze a low-complexity channel estimator for a multiuser multicarrier code division multiple access (MC-CDMA) downlink in a time-variant frequency-selective channel. MC-CDMA is based on orthogonal frequency division multiplexing (OFDM). The time-variant channel is estimated individually for every flat-fading subcarrier, assuming small intercarrier interference. The temporal variation of every subcarrier over the duration of a data block is upper bounded by the Doppler bandwidth determined by the maximum velocity of the users. Slepian showed that time-limited snapshots of bandlimited sequences span a low-dimensional subspace. This subspace is also spanned by discrete prolate spheroidal (DPS) sequences. We expand the time-variant subcarrier coefficients in terms of orthogonal DPS sequences we call Slepian basis expansion. This enables a time-variant channel description that avoids the frequency leakage effect of the Fourier basis expansion. The square bias of the Slepian basis expansion per subcarrier is three magnitudes smaller than the square bias of the Fourier basis expansion. We show simulation results for a fully loaded MC-CDMA downlink with classic linear minimum mean square error multiuser detection. The users are moving with 19.4 m/s. Using the Slepian basis expansion channel estimator and a pilot ratio of only 2%, we achieve a bit error rate performance as with perfect channel knowledge.

Index Terms—Discrete prolate spheroidal sequence, MC-CDMA, OFDM, Slepian basis expansion, time-variant channel estimation.

I. INTRODUCTION

THIS paper describes a solution for the problem of channel estimation in a wireless communication system based on multicarrier (MC) code division multiple access (CDMA) when users are moving at vehicular speed. MC-CDMA is based on orthogonal frequency division multiplexing (OFDM), and the data symbols are spread by a user specific spreading sequence that is applied in the frequency domain. The transmission scheme is block oriented. A block consists of OFDM data symbols with interleaved OFDM pilot symbols to allow pilot-based estimation of the time-variant channel.

OFDM transforms the time-variant frequency-selective channel into a set of time-variant frequency-flat subcarriers. We deal with time-variant channels that vary significantly over the duration of a long block of OFDM symbols. Each OFDM symbol is preceded by a cyclic prefix to avoid intersymbol interference.

The variation of a wireless channel over the duration of a data block is caused by several impinging wavefronts, each with potentially different Doppler shifts. The Doppler frequencies depend on the velocity, the carrier frequency f_C, and the scattering environment. The maximum variation in time of the wireless channel is upper bounded by the maximum normalized one-sided Doppler bandwidth

$$\nu_{\mathrm{Dmax}} = \frac{v_{\max} f_C}{c_0} T_S \qquad (1)$$

where $v_{\max}$ is the maximum (supported) velocity, T_S is the OFDM symbol duration, and c_0 is the speed of light.

Under the assumption of small intercarrier interference (ICI), each time-variant frequency-flat subcarrier is fully described through a sequence of complex scalars at the OFDM symbol rate $1/T_S$. This sequence is bandlimited by ν_{Dmax}. At the receiver side, we perform block-oriented processing for data detection and channel estimation. Hence, we aim at finding a channel representation that describes a time-variant subcarrier for the duration of a single data block.

In [1] and [2], the autocorrelation of the channel, i.e., its second-order statistic, is assumed to be known, and a Kalman filter or a Karhunen–Loéve transform are applied. The autocorrelation is calculated under the assumption of a dense scatterer model in the limit of an infinite number of scatterers [3], [4, Sec. 2.5.2]. This assumption is *not* fulfilled in practical channels [5]. Furthermore, the actual velocity of the user and the angles of arrival enter the autocorrelation as parameters and must be estimated explicitly. Another approach along these lines is to estimate and track the channel statistics online [6].

We estimate the parameters of a deterministic channel model from a single realization of a randomly fading channel using known pilot symbols. The discrete multipath channel model discussed in [7] is a deterministic channel description that depends nonlinearly on the Doppler frequencies of each propagation path. We want to avoid such a nonlinear estimation problem [8], [9].

We use a basis expansion with an appropriately chosen set of basis functions to describe the variation of the channel in time. Fourier basis functions are applied in [10] and [11] to represent the time-variant channel. We have observed that the

Fourier basis expansion, i.e., a truncated discrete Fourier transform (DFT), has the following major drawback: the rectangular window associated with the DFT introduces spectral leakage [12, Sec. 5.4]. The energy from low-frequency Fourier coefficients leaks to the full frequency range. When the DFT is truncated, an effect similar to the Gibbs phenomenon [12, Sec. 2.4.2], together with spectral leakage, leads to significant phase and amplitude errors at the beginning and at the end of the data block [4]. This results in a floor in the bit error rate (BER) for channels with Doppler spread, as was shown in [13] and [14].

The Slepian basis expansion represents bandlimited sequences with a minimum number of basis functions avoiding the deficiencies of the Fourier basis expansion. Slepian showed in [15] that time-limited parts of bandlimited sequences span a low-dimensional subspace. The orthogonal basis is spanned by the so-called discrete prolate spheroidal (DPS) sequences. These DPS sequences have a *double* orthogonality property: They are orthogonal over the *finite* set $\{0, \ldots, M-1\}$ and the *infinite* set $\{-\infty, \ldots, \infty\} = \mathbb{Z}$ simultaneously. This remarkable property enables parameter estimation without the drawbacks of windowing in the case of the Fourier basis expansion [15, Sec. 3.1.4]. The basis functions of the Slepian basis expansion are bandlimited to the known maximum variation in time of the channel ν_{Dmax} and time-concentrated for the duration of the transmitted data block with length M [16].

A. Contributions

- We apply the concept of discrete prolate spheroidal sequences for the estimation of time-variant mobile communication channels.
- We compare the channel estimation square bias and variance of the Slepian basis expansion and the Fourier basis expansion for time-variant flat-fading channels. Analytical expressions are established for time-variant channels with arbitrary Doppler spectra of finite support. Numerical simulations are carried out for time-variant channels with Jakes' Doppler spectrum [17] and compared with the analytical results.
- We develop a low-complexity channel estimator for a MC-CDMA downlink in a time-variant frequency-selective channel. This estimator does *not* need detailed knowledge of the channels autocorrelation (i.e., the Doppler spectrum).
- We show simulation results for a fully loaded MC-CDMA downlink with classic linear minimum mean square error (MMSE) multiuser detection [18]. The users are moving with 19.4 m/s. Using the Slepian basis expansion channel estimator and a pilot ratio of only 2%, we achieve a bit error rate performance as with perfect channel knowledge.

B. Paper Organization

To simplify the initial presentation, we define a signal model for a time-variant flat-fading channel in Section III. In Section IV, the properties of the DPS sequences are described, and the associated Slepian basis expansion for time-variant flat-fading channel estimation is defined. We give an analytical and numerical performance evaluation of the time-variant

flat-fading channel estimation error for the Slepian basis expansion and the Fourier basis expansion in Section V. In Section VI, the MC-CDMA system is introduced, and we generalize our channel estimator to time-variant frequency-selective channels. The performance results of the Slepian basis expansion are compared with the one obtained with the Fourier basis expansion. Finally, we conclude in Section VII.

II. NOTATION

$\boldsymbol{a}$	Column vector with elements $a[i]$.
$\boldsymbol{A}$	Matrix with elements $[\boldsymbol{A}]_{i,\ell}$.
$\boldsymbol{A}_{P \times Q}$	Upper left part of $\boldsymbol{A}$ with dimension $P \times Q$.
$\boldsymbol{A}^T$	Transpose of $\boldsymbol{A}$.
$\boldsymbol{A}^H$	Conjugate transpose of $\boldsymbol{A}$.
$\mathrm{diag}(\boldsymbol{a})$	Diagonal matrix with entries $a[i]$.
$\boldsymbol{I}_Q$	$Q \times Q$ identity matrix.
$\boldsymbol{1}_Q$	$Q \times 1$ column vector with all ones.
$\boldsymbol{o}_Q$	$Q \times 1$ column vector with all zeros.
a^*	Complex conjugate of a.
$|a|$	Absolute value of a.
$\lfloor a \rfloor$	Largest integer, lower or equal than $a \in \mathbb{R}$.
$\lceil a \rceil$	Smallest integer, greater or equal than $a \in \mathbb{R}$.
$\|\boldsymbol{a}\|$	ℓ_2-norm of vector $\boldsymbol{a}$.
δ_{ij}	1 for $i = j$, 0 otherwise.

III. SIGNAL MODEL FOR FLAT-FADING TIME-VARIANT CHANNELS

We consider the transmission of a symbol sequence $d[m]$ with symbol rate $R_S = 1/T_S$ over a time-variant flat-fading channel in order to simplify the initial presentation. The symbol duration is much longer than the delay spread of the channel $T_S \gg T_D$. Discrete time is denoted by m. The channel in equivalent baseband notation $h(t, \tau)$ incorporates the transmit filter, the physical channel, and the matched receive filter. The received sequence $y[m]$ is given by the multiplication of the symbol sequence and the sampled time-variant channel $h[m] \triangleq h(mT_S, 0)$ plus additional circular symmetric complex white Gaussian noise $z[m]$ with zero mean and variance σ_z^2

$$y[m] = h[m]d[m] + z[m], \quad m \in \{0, \ldots, M-1\}. \quad (2)$$

We transmit symbols in blocks of length M. Each block consists of $M - J$ data symbols $b[m]$ with J interleaved pilot symbols $p[m]$

$$d[m] = b[m] + p[m]. \quad (3)$$

The data symbols satisfy $b[m] \in \{\pm 1 \pm j\}/\sqrt{2}$ for $m \notin \mathcal{P}$ and $b[m] = 0$ for $m \in \mathcal{P}$.

The pilot symbols are independent identically distributed (i.i.d.) chosen with equal probability from the QPSK symbol set $p[m] = \{\pm 1 \pm j\}/\sqrt{2}$ for $m \in \mathcal{P}$ and $p[m] = 0$ for $m \notin \mathcal{P}$. The pilot placement is defined through the index set

$$\mathcal{P} = \left\{ \left\lfloor i\frac{M}{J} + \frac{M}{2J} \right\rfloor \mid i \in \{0, \ldots, J-1\} \right\}. \quad (4)$$

Fig. 1 shows an example for the pilot set $\mathcal{P}$ defined in (4). The optimal pilot placement is not known to the authors; however, a
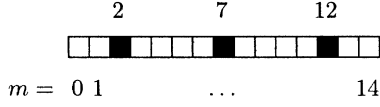
Fig. 1. Example pilot pattern $\mathcal{P} = \{2, 7, 12\}$ defined by (4) for $M = 15$ and $J = 3$.

uniform placement performs well as shown below. The symbols have constant modulus, their energy is normalized $|d[m]| = \sqrt{E_S} = 1$.

For channel estimation and equalization at the receiver, we need an efficient representation of the channel $h[m]$ for $m \in \{0, \ldots, M-1\}$. The theory of time-concentrated and bandlimited sequences developed by Slepian [15] enables a new approach for the time-variant channel estimation problem, which we will pursue in Section IV. We will exploit the knowledge of two parameters only: the maximum Doppler bandwidth ν_{Dmax} and the block length M.

IV. SLEPIAN BASIS EXPANSION

Slepian [15] answered the question of which sequences are bandlimited to the frequency range $[-\nu_{\mathrm{Dmax}}, \nu_{\mathrm{Dmax}}]$ and simultaneously most concentrated in a certain time interval of length M. The sequences $u[m]$ we are seeking will have their maximum energy concentration in an interval with length M

$$\lambda(\nu_{\mathrm{Dmax}}, M) = \frac{\sum_{m=0}^{M-1} |u[m]|^2}{\sum_{m=-\infty}^{\infty} |u[m]|^2} \quad (5)$$

while being bandlimited to ν_{Dmax}; hence

$$u[m] = \int_{-\nu_{\mathrm{Dmax}}}^{\nu_{\mathrm{Dmax}}} U(\nu) e^{j2\pi m\nu} d\nu \quad (6)$$

where

$$U(\nu) = \sum_{m=-\infty}^{\infty} u[m] e^{-j2\pi m\nu}. \quad (7)$$

We see that $0 \le \lambda(\nu_{\mathrm{Dmax}}, M) \le 1$.

The solution of this constrained maximization problem are the discrete prolate spheroidal (DPS) sequences [15]. The DPS sequences $u_i^{(S)}[m, \nu_{\mathrm{Dmax}}, M]$ are defined as the real-valued solution of

$$\sum_{\ell=0}^{M-1} \frac{\sin(2\pi\nu_{\mathrm{Dmax}}(\ell-m))}{\pi(\ell-m)} u_i^{(S)}[\ell, \nu_{\mathrm{Dmax}}, M]$$
$$= \lambda_i(\nu_{\mathrm{Dmax}}, M) u_i^{(S)}[m, \nu_{\mathrm{Dmax}}, M] \quad (8)$$

for $i \in \{0, \ldots, M-1\}$ and $m \in \{-\infty, \ldots, \infty\}$ [15]. We drop the explicit dependence of $u_i^{(S)}[m]$ and λ_i on ν_{Dmax} and M, which we consider fixed system parameters for the remainder of the paper.

The DPS sequence $u_0[m]$ is the unique sequence that is band-limited and most time-concentrated in a given interval with length M, $u_1[m]$ is the next sequence having maximum energy concentration among the DPS sequences orthogonal to $u_0[m]$, and so on. Thus, the DPS sequences show that a set

of orthogonal sequences exists that is exactly bandlimited and simultaneously posses a high (but not complete) time concentration in a certain interval with length M. The eigenvalues λ_i are a measure for this energy concentration expressed by (5).

The DPS sequences are doubly orthogonal on the infinite set $\{-\infty, \ldots, \infty\} = \mathbb{Z}$ and the finite set $\{0, \ldots, M-1\}$. More specifically

$$\sum_{m=0}^{M-1} u_i^{(S)}[m] u_j^{(S)}[m] = \lambda_i \sum_{m=-\infty}^{\infty} u_i^{(S)}[m] u_j^{(S)}[m] = \delta_{ij} \quad (9)$$

where $i, j \in \{0, \ldots, M-1\}$. This means that the DPS sequences are orthonormal on the set $m \in \{0, \ldots, M-1\}$ and orthogonal on the set $m \in \{-\infty, \ldots, \infty\} = \mathbb{Z}$. The eigenvalues λ_i are clustered near 1 for $i \le \lceil 2\nu_{\mathrm{Dmax}} M \rceil$ and rapidly drop to zero for $i > \lceil 2\nu_{\mathrm{Dmax}} M \rceil$. Therefore, the signal space dimension [15, Sec. 3.3] of time-limited snapshots of a bandlimited signal is approximately given by

$$D' = \lceil 2\nu_{\mathrm{Dmax}} M \rceil + 1. \quad (10)$$

For a rigorous proof, see [19]. All the properties described so far enable parameter estimation without the drawbacks of windowing as in the case of the Fourier basis expansion [15, Sec. 3.3].

For our application, we are interested in $u_i^{(S)}[m]$ for the time index set $m \in \{0, \ldots, M-1\}$ only. We introduce the term Slepian sequences for the index limited DPS sequences and define the vector $\boldsymbol{u}_i^{(S)} \in \mathbb{R}^M$ with elements $u_i^{(S)}[m]$ for $m \in \{0, \ldots, M-1\}$. The Slepian sequences $\boldsymbol{u}_i^{(S)}$ are eigenvectors of the matrix $\boldsymbol{C} \in \mathbb{R}^{M \times M}$, fulfilling

$$\boldsymbol{C} \boldsymbol{u}_i^{(S)} = \lambda_i \boldsymbol{u}_i^{(S)}. \quad (11)$$

The eigenvalues λ_i are identical to those in (8). Matrix $\boldsymbol{C}$ is defined as

$$[\boldsymbol{C}]_{i,\ell} = \frac{\sin[2\pi(i-\ell)\nu_{\mathrm{Dmax}}]}{\pi(i-\ell)} \quad (12)$$

where $i, \ell \in \{0, \ldots, M-1\}$.

Concluding, the Slepian sequences span an orthonormal basis that allows the representation of a time-limited snapshot of bandlimited sequences through a basis expansion. The Slepian basis expansion expands the sequence $h[m]$ in terms of Slepian sequences $u_i^{(S)}[m]$

$$h[m] \approx \tilde{h}^{(S)}[m] = \sum_{i=0}^{D^{(S)}-1} u_i^{(S)}[m] \gamma_i^{(S)} \quad (13)$$

where $m \in \{0, \ldots, M-1\}$. The dimension of this basis expansion fulfills

$$D' \le D^{(S)} \le M. \quad (14)$$

Wherever possible, we will use a generic notation for the basis expansion quantities $u_i[m]$, D, γ_i, and $\tilde{h}[m]$ to indicate that the expression is applicable to any set of orthonormal basis functions $u_i[m]$. If we specifically want to reference the Slepian basis expansion, we use the superscript $(\cdot)^{(S)}$. In Fig. 2, the DPS
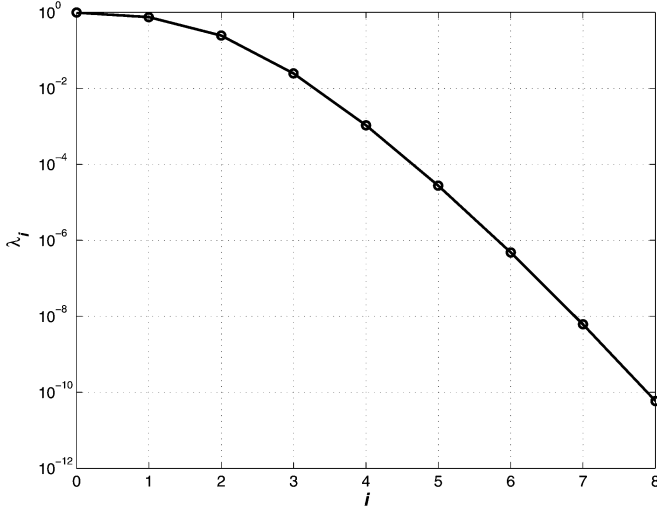
Fig. 2. Eigenvalue spectrum λ_i for the Slepian sequences. The Slepian sequences are designed for block length $M = 256$ and a maximum Doppler bandwidth $\nu_{\mathrm{Dmax}} = 3.9 \cdot 10^{-3}$. The approximate dimension of the signal space evaluates to $D' = \lceil 2\nu_{\mathrm{Dmax}} M \rceil + 1 = 3$.
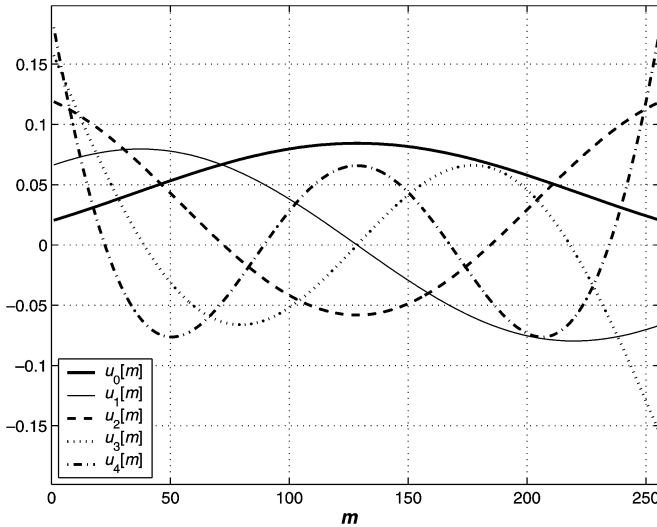

Fig. 3. Slepian sequences $u_i^{(S)}[m]$ for block length $M = 256$ and maximum normalized Doppler bandwidth $\nu_{\mathrm{Dmax}} = 3.9 \cdot 10^{-3}$.

eigenvalue spectrum is given. The Slepian sequences $\boldsymbol{u}_i^{(S)}$ for $i \in \{0, \dots, 4\}$ are depicted in Fig. 3.

By choosing D, we can control the mean square error (MSE) of the basis expansion defined as

$$\mathrm{MSE}_M = \frac{1}{M} \sum_{m=0}^{M-1} \mathbb{E}\{|h[m] - \tilde{h}[m]|^2\}. \tag{15}$$

In order to highlight the utility of the Slepian basis expansion in terms of dimension reduction, we give a numerical example of an actual communication system. We use the following parameters: carrier frequency $f_C = 2$ GHz, symbol rate $1/T_S = 48.6 \cdot 10^3 \ \mathrm{s}^{-1}$, maximum speed of the user $v_{\mathrm{max}} = 102.5 \ \mathrm{km/h} = 28.5 \ \mathrm{m/s}$, maximum normalized Doppler frequency $\nu_{\mathrm{Dmax}} = 3.9 \cdot 10^{-3}$, and data block length $M = 256$. With these system parameters, the approximate

dimension of the signal space $D' = \lceil 2\nu_{\mathrm{Dmax}} M \rceil + 1 = 3$. Therefore, the dimension of the estimation problem is reduced by a factor of $256/3 = 85$, which is a very considerable saving.

The pilot pattern $\mathcal{P}$ in our application allows us to obtain channel knowledge for $m \in \mathcal{P}$. We define the vector

$$\boldsymbol{f}[m] = \begin{bmatrix} u_0[m] \\ \vdots \\ u_{D-1}[m] \end{bmatrix} \in \mathbb{R}^D \tag{16}$$

with the instantaneous values of the basis functions and the correlation matrix

$$\boldsymbol{G} = \sum_{l \in \mathcal{P}} \boldsymbol{f}[l] \boldsymbol{f}^H[l] \tag{17}$$

where we have used the fact that $|p[m]| = \sqrt{E_S} = 1$. The basis expansion parameters in (13) are estimated according to

$$\hat{\boldsymbol{\gamma}} = \boldsymbol{G}^{-1} \sum_{m \in \mathcal{P}} y[m] p^*[m] \boldsymbol{f}^*[m] \tag{18}$$

where

$$\hat{\boldsymbol{\gamma}} = [\hat{\gamma}_0, \dots, \hat{\gamma}_{(D-1)}]^T. \tag{19}$$

We use a generic notation since (16)–(18) are valid for any basis expansion.

V. BASIS EXPANSION ERROR ANALYSIS FOR TIME-VARIANT FLAT-FADING CHANNELS

To demonstrate the merits of the Slepian basis expansion, we compare its performance to the Fourier basis expansion by means of simulations with the system defined in (2). Additionally, we will compare the simulation results with analytic results derived in Sections V-B and C.

A. Channel Model and System Assumption

The actual realization of the time-variant flat-fading channel $h[m]$ is calculated according to the simulation model in the Appendix. The autocorrelation of $h[m]$ is

$$\mathbb{E}\{h^*[m + \tilde{m}]h[m]\} = R_{hh}[\tilde{m}] = J_0(2\pi\nu_D \tilde{m}) \tag{20}$$

where J_0 is the zeroth-order Bessel function of the first kind, and

$$\nu_D = \frac{v f_C}{c_0} T_S \tag{21}$$

is the one-sided normalized Doppler bandwidth in the range $0 \le \nu_D < \nu_{\mathrm{Dmax}}$. The true speed of the user is denoted by v, with $|v| < v_{\mathrm{max}}$.

The symbol duration $T_S = (64 + 15)/(3.84 \cdot 10^6 \ \mathrm{s}^{-1}) = 20.57 \ \mu s$ is chosen for later comparison with the MC-CDMA system introduced in Section VI. The speed of the user is varied in the range $0 < v < v_{\mathrm{max}} = 100 \ \mathrm{km/h} = 27.8 \ \mathrm{m/s}$, which results in a range of Doppler bandwidths $0 \le B_D \le 180$ Hz

or normalized to the symbol duration $0 \leq \nu_D \leq 3.8 \cdot 10^{-3}$. The length of the data block is $M = 256$ symbols, and the time index is restricted to $0 \leq m \leq M - 1$. All basis expansions use the same amount of parameters to model the channel $D^{(S)} = D^{(F)} = 5$.

The MSE (15) of the basis expansion can be described by the sum of a square bias and a variance term

$$\text{MSE}_M = \text{bias}_M^2 + \text{var}_M. \qquad (22)$$

We will see in Section V-B that bias_M^2 depends on the actual set of basis functions, and var_M depends linearly on the noise variance σ_z^2 and the dimension D of the basis expansion.

B. Basis Expansion Square Bias

Using Niedzwiecki's results from [4, Sec. 6] and specializing to our application, we obtain an analytic expression for the basis expansion square bias. We define the instantaneous frequency response of the basis expansion estimator according to

$$H[m, \nu] = \boldsymbol{f}^T[m] \boldsymbol{G}^{-1} \sum_{\ell \in \mathcal{P}} \boldsymbol{f}^*[\ell] e^{-j2\pi\nu(m-\ell)} \qquad (23)$$

where $m \in \{0, \dots, M - 1\}$, and $|\nu| < 1/2$.

In (23), the sum $\sum_{\ell \in \mathcal{P}} \boldsymbol{f}^*[\ell] e^{-j2\pi\nu(m-\ell)}$ projects the complex exponential onto the basis function at the pilot grid positions, i.e., we calculate the inner product with every basis function. Then, the realization at time instant m is calculated by left multiplying with $\boldsymbol{f}^T[m]$.

The complex exponential in (23) is shifted by m; thus, $|H[m, \nu]|$ is the instantaneous amplitude response of the basis expansion at time instant m. The phase of $H[m, \nu]$, which is expressed by $\arg(H[m, \nu])$, is the instantaneous phase shift of the basis expansion at time index m. The design goal for a basis expansion is to have no amplitude error $|H[m, \nu]| = 1$ and no phase error $\arg(H[m, \nu]) = 0$. Therefore, the instantaneous error characteristic of the basis expansion is defined as [4, Sec. 6.1.4]

$$E[m, \nu] = |1 - H[m, \nu]|^2. \qquad (24)$$

The square bias per symbol $\text{bias}^2[m]$ of the basis expansion estimator can be expressed as the integral over the instantaneous error characteristic $E[m, \nu]$ multiplied by the power spectral density of $h[m]$ (see [4, Sec. 6.1.4])

$$\text{bias}^2[m] = \int_{-(1/2)}^{1/2} E[m, \nu] S_{hh}(\nu) D\nu \qquad (25)$$

where $S_{hh}(\nu)$ is given by

$$S_{hh}(\nu) = \sum_{\tilde{m}=-\infty}^{\infty} R_{hh}[\tilde{m}] e^{-j2\pi\tilde{m}\nu}. \qquad (26)$$

The square bias for a block of length M is given by

$$\text{bias}_M^2 = \frac{1}{M} \sum_{m=0}^{M-1} \text{bias}^2[m]. \qquad (27)$$

In order to obtain analytic performance results, we evaluate the basis expansion estimator for the autocorrelation defined in (20), which corresponds to the Jakes' spectrum

$$S_{hh}(\nu) = \frac{1}{\pi\nu_D \sqrt{1 - \left(\frac{\nu}{\nu_D}\right)^2}}, \text{ for } |\nu| < \nu_D \qquad (28)$$

and $S_{hh}(\nu) = 0$ elsewhere. Inserting (28) in (25) and calculating the integral numerically, we plot the results after evaluating (27) in Fig. 4. The results for the Slepian basis expansion are obtained by using $u_i^{(S)}[m]$ in (16), and for the Fourier basis expansion, we substitute

$$u_i^{(F)}[m] = \frac{1}{\sqrt{M}} e^{(j2\pi(i-(D-1)/2)m/M)} \qquad (29)$$

into (16).

Note that the Slepian basis expansion estimator only exploits that $S_{hh}(\nu) = 0$ for $|\nu| > \nu_{\text{Dmax}}$ and does *not* require any other knowledge about the Doppler spectrum of the time-variant channel for the design of the basis functions. The design parameters for our Slepian basis expansion are ν_{Dmax} and M. *Only* to allow for easier comparison with other publications, we use the autocorrelation (20). Real channels do *not* show Jakes' Doppler spectrum, as was proven by measurements in [5]. In fact, with (25), we are able to evaluate the basis expansion estimator square bias for any autocorrelation. To achieve optimum performance with the Slepian basis expansion, the power spectral density must fulfill

$$S_{hh}(\nu) = 0, \text{ for } \nu_{\text{Dmax}} \leq |\nu| < \frac{1}{2} \qquad (30)$$

which is ensured by the physical mechanism behind the Doppler effect in a wireless channel.

The numerical square bias results are obtained using the signal model defined in Section III for $\sigma_z^2 = 0$. We average over 2000 channel realizations of the channel defined in Section V-A. The channel estimation is performed according to (18). Using the reconstruction expression (13) and evaluating (15) in the sense of an empirical mean provides the numerical square bias results under the condition $\sigma_z^2 = 0$. Fig. 4 plots the square bias of the the Slepian basis expansion and the Fourier basis expansion for $0 \leq \nu_D \leq 3.8 \cdot 10^{-3}$ and $J = 10$ pilots. The simulation results in terms of bias_M^2 versus normalized Doppler bandwidth ν_D are given in Fig. 4, together with the analytic results that show a perfect match. The square bias of the Slepian basis expansion is three magnitudes smaller if compared with the Fourier basis expansion. The square bias of the Fourier basis expansion slightly decays toward $\nu_{\text{Dmax}} = 3.9 \cdot 10^{-3} = 1/M = 1/256$ since this frequency coincides with the one of the Fourier basis function and, thus, is a local minimum. The same behavior is also visible in Fig. 6. Similar performance results for the Fourier basis expansion are reported in [21] as well.

In [22], a set of nonorthogonal complex exponential basis functions $e^{j2\pi\nu_i m}$ with $|\nu_i| \leq \nu_{\text{Dmax}}$ and $m \in \{0, \dots, M - 1\}$ is used. This basis spans an approximation of the Slepian subspace by definition. We depict its square bias after an orthog-
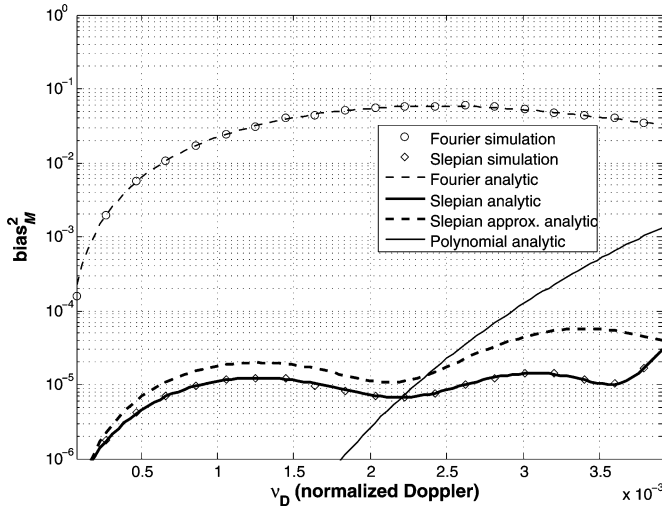
Fig. 4. bias^2_M for the Fourier and the Slepian basis expansion with dimension $D^{(F)} = D^{(S)} = 5$ and $J = 10$ pilots. We vary the Doppler bandwidth in the range $0 \leq \nu_D \leq 3.8 \cdot 10^{-3}$. Additionally, we depict the square bias for the polynomial approach of [20] (denoted "Polynomial") and the nonorthogonal complex exponentials used in [11] (denoted "Slepian approx."), both with five basis functions.
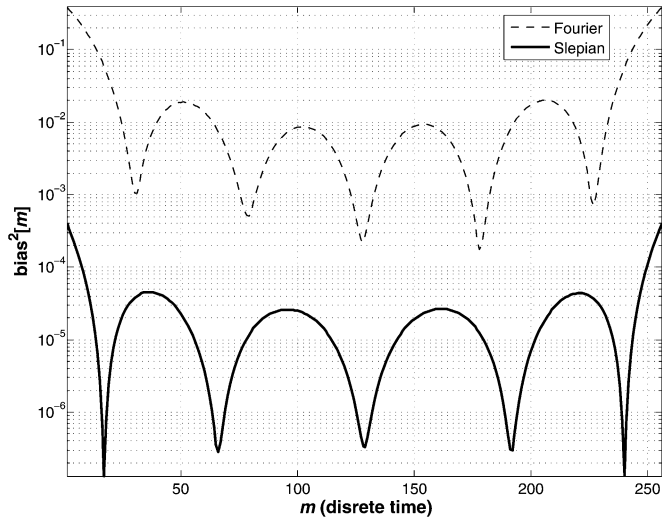

Fig. 5. Square bias per symbol $\text{bias}^2[m]$ for the Fourier and the Slepian basis expansion with dimension $D^{(F)} = D^{(S)} = 5$, $J = 10$ pilots, and $v = 27.8$ m/s.

onalization step in Fig. 4 (denoted "Slepian approx.") for five basis functions.

A polynomial approach resulting from a Taylor expansion was used in [20]. This basis is not restricted to time-limited and bandlimited functions. Thus, its square bias varies heavily over the normalized Doppler range of interest, as shown in Fig. 4 (denoted "Polynomial") for five basis functions.

The Slepian basis expansion needs fewer parameters and shows better performance than the spline approximation investigated in [23].

Fig. 5 plots the analytic result for the square bias per symbol (25). This shows clearly that the square bias per symbol of the Fourier basis expansion is highest at the edges of the data block. The square bias curve of the Slepian basis expansion has the same qualitative behavior toward the block boundaries, but the
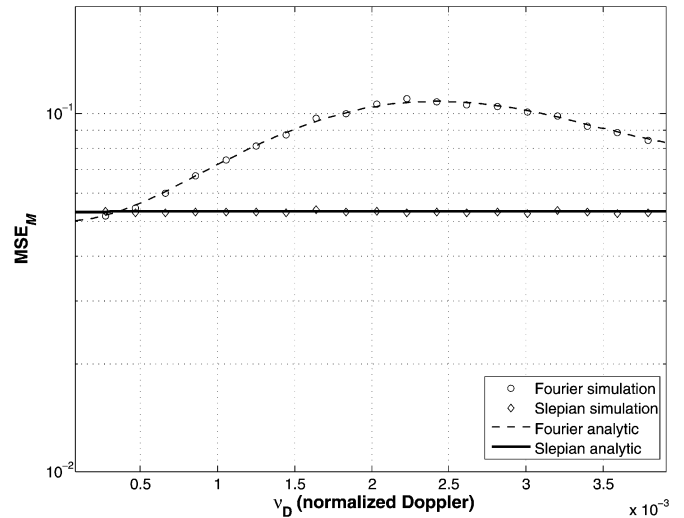

Fig. 6. MSE_M of the basis expansion estimator with $J = 10$ pilot symbols at an $E_S/N_0 = 10$ dB for one user moving with $v = 0 \ldots 27.8$ m/s corresponding to $\nu_D = 0 \ldots 3.8 \cdot 10^{-3}$.

square bias per symbol of the Slepian basis expansion is several magnitudes lower compared to the Fourier basis expansion.

C. Basis Expansion Variance

For channel estimation purposes, we define

$$\frac{E_S}{N_0} = \frac{1}{\sigma_z^2}. \tag{31}$$

Note that this definition is different from E_b/N_0, which we will use later for data detection, cf. (50). Using the results from [4, Sec. 6.1.4], we can express the basis expansion estimator variance as

$$\text{var}_M \approx \sigma_z^2 \frac{1}{M} \sum_{m=0}^{M-1} \boldsymbol{f}^H[m] \boldsymbol{G}^{-1} \boldsymbol{f}[m] \approx \sigma_z^2 \frac{D}{J}. \tag{32}$$

Equation (32) becomes exact for $\text{bias}^2_M = 0$. Thus, var_M increases with the dimension of the basis expansion D and decreases with an increasing number of pilot symbols J but does not depend on the block length M.

Fig. 6 evaluates the basis expansion estimator for a signal-to-noise ratio of $E_S/N_0 = 10$ dB, $J = 10$ pilot symbols, and $0 \leq \nu_D \leq 3.8 \cdot 10^{-3}$. The square bias of the Fourier basis expansion dominates the MSE (22), and the distance to the Slepian basis expansion is reduced because of the present noise level of $E_S/N_0 = 10$ dB.

Fig. 7 plots the analytic and simulation results for a varying number of pilot symbols $J \in \{5, \ldots, 15\}$ with $\nu_D = 3.8 \cdot 10^{-3}$ and $E_S/N_0 = 15$ dB. The MSE of the Slepian basis expansions is smaller than the MSE of the Fourier basis expansion.

Finally, we fix $J = 10$ and $\nu_D = 3.8 \cdot 10^{-3}$ and vary E_S/N_0 in the range of 0 to 30 dB. Fig. 8 shows that the Fourier basis expansion is biased and that its MSE saturates for increasing E_S/N_0 at $3.5 \cdot 10^{-2}$. The Slepian basis expansion is (practically) unbiased. The error floor of the Fourier basis expansion can be explained due to the structure of (22). With increasing E_S/N_0, the variance var_M(32) decreases, and the square bias
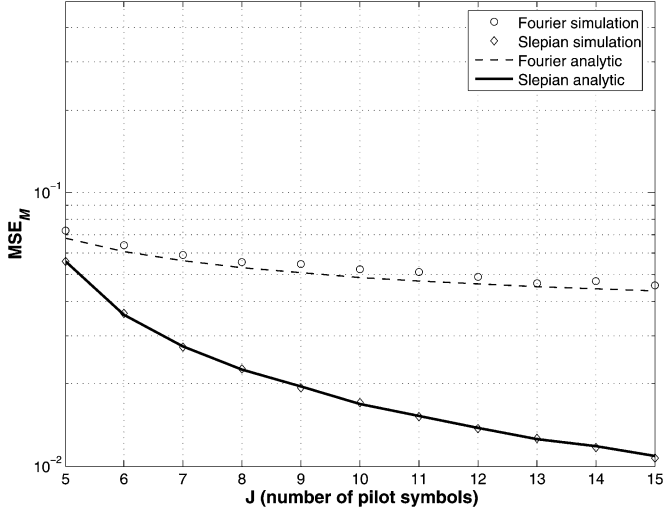
Fig. 7. MSE_M of the basis expansion estimator with $J \in \{5, \ldots, 15\}$ pilot symbols at an $E_S/N_0 = 15$ dB for one user moving with $v = 27.8$ m/s corresponding to $\nu_D = 3.8 \cdot 10^{-3}$.
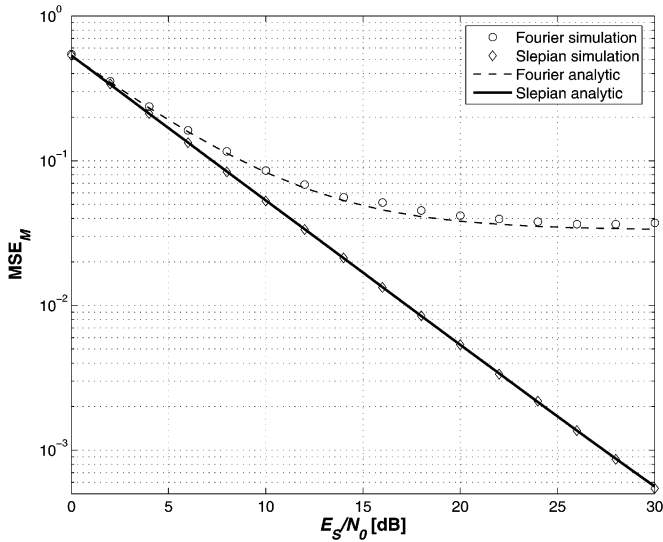

Fig. 8. MSE_M of the basis expansion estimator for $J = 10$ pilot symbols at an $E_S/N_0 = 0 \ldots 30$ dB for one user moving with $v = 27.8$ m/s corresponding to $\nu_D = 3.8 \cdot 10^{-3}$.

bias_M^2 (27) starts to dominate the MSE since it is independent of E_S/N_0.

From this analysis, it is clear that the Slepian basis expansion offers major performance gains compared with the Fourier basis expansion while having the same complexity.

VI. MC-CDMA FOR TIME-VARIANT FREQUENCY-SELECTIVE CHANNELS

In this section, we define the signal model for a MC-CDMA downlink in a time-variant channel, the linear MMSE multiuser detector, and the Slepian basis expansion channel estimator. We provide simulation results showing that this system needs a pilot ratio of 2% only, in order to achieve the same performance as with perfect channel knowledge.

A. Signal Model

In MC-CDMA, a data symbol is spread by a user-specific spreading code. The resulting chips are processed by an inverse DFT to obtain an OFDM symbol. The transmission is block oriented. A data block consists of $M - J$ OFDM data symbols and J OFDM pilot symbols. Every OFDM symbol is preceded by a cyclic prefix to avoid ISI. The channel varies significantly over the duration of a long data block.

The base station transmits quaternary phase shift keying (QPSK) modulated symbols $b_k[m]$ with symbol rate $R_S = 1/T_S$. There are K users in the system, and the user index is denoted by k. Each symbol is spread by a random spreading sequence $s_k \in \mathbb{C}^N$ with elements $\{\pm 1 \pm j\}/\sqrt{2N}$. Fig. 9 depicts the downlink transmitter schematically. The data symbols $b_k[m]$ result from the binary information sequence $\chi_k[m'']$ of length $2(M - J)R_C$ by convolutional encoding with code rate R_C, random interleaving, and QPSK modulation with Gray labeling.

In order to accommodate for time-variant channel estimation, the $M - J$ data symbols are distributed over a block of length M, allowing for pilot symbol insertion. Thus, the data symbols satisfy $b_k[m] \in \{\pm 1 \pm j\}/\sqrt{2}$ for $m \notin \mathcal{P}$ and $b_k[m] = 0$ for $m \in \mathcal{P}$, where the pilot placement is defined through (4). We ignore the effects of path loss and shadow fading

$$\alpha_k = 1, \text{ for } k \in \{1, \ldots, K\} \qquad (33)$$

and a perfect power control is assumed. As shown in Fig. 9, the spread signals of all users are added together, and common pilot symbols $\boldsymbol{p}[m] \in \mathbb{C}^N$ with elements $p[m, q]$ are added

$$\boldsymbol{d}[m] = \boldsymbol{S}\boldsymbol{b}[m] + \boldsymbol{p}[m] \qquad (34)$$

where

$$\boldsymbol{S} = [\boldsymbol{s}_1, \ldots, \boldsymbol{s}_K] \in \mathbb{C}^{N \times K} \qquad (35)$$

and

$$\boldsymbol{b}[m] = [b_1[m], \ldots, b_K[m]]^T \in \mathbb{C}^K \qquad (36)$$

contains the stacked data symbols for K users. The elements of the pilot symbol vector $p[m, q]$ for $m \in \mathcal{P}$ and $q \in \{0, \ldots, N - 1\}$ are i.i.d. chosen with equal probability from the scaled QPSK symbol set $K\{\pm 1 \pm j\}/\sqrt{2N}$; otherwise, $\boldsymbol{p}[m] = \mathbf{o}_N$ for $m \notin \mathcal{P}$.

Then, an N-point inverse DFT is performed, and a cyclic prefix of length G is inserted [24]. The OFDM symbol including the cyclic prefix has length $P = N + G$. After parallel serial conversion, the chip stream $\mu[n]$ with chip rate $1/T_C = P/T_S$ is transmitted over a time-variant multipath fading channel $h(t, \tau)$. We denote the chip-rate sampled time-variant impulse response by

$$h'[n, \ell] = h(nT_C, \ell T_C). \qquad (37)$$

A time-variant channel impulse response generally introduces intercarrier interference in an OFDM system. However, if the channel variation in time, measured by the normalized
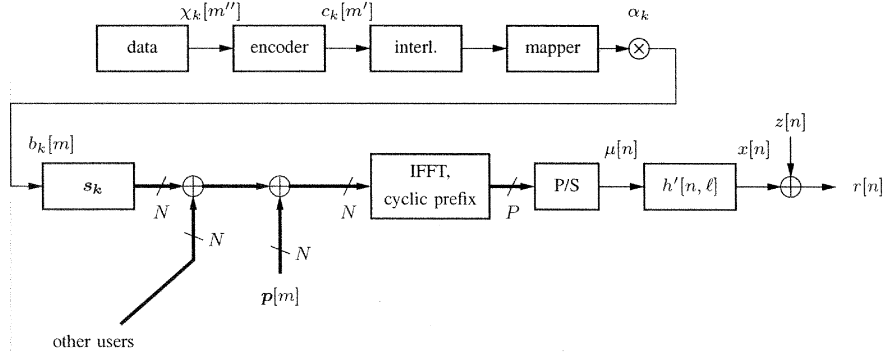
Fig. 9.   Model for the MC-CDMA transmitter and the channel in the time-variant downlink.

Doppler bandwidth, stays below a certain threshold, the intercarrier interference can be neglected for the receiver side processing [25]. This threshold is fulfilled if the one-sided normalized Doppler bandwidth ν_D is much smaller than the normalized subcarrier bandwidth P/N

$$\frac{\nu_D N}{P} < \epsilon. \tag{38}$$

For $\epsilon = 10^{-2}$, the DFT is still applicable [26], although the channel is time variant.

For the processing at the receiver side, we are able to treat the time-variant channel as constant for the duration of each single OFDM symbol if (38) is fulfilled. Hence

$$h[m, \ell] = h'[mP, \ell] \tag{39}$$

respectively

$$\boldsymbol{h}[m] = [h[m, 0], \dots, h[m, L-1]]^T \in \mathbb{C}^{L \times 1} \tag{40}$$

in vector notation. The time-variant frequency response $\boldsymbol{g}[m] \in \mathbb{C}^N$ with elements $g[m, q]$ is defined as the DFT of the time-variant impulse response

$$\boldsymbol{g}[m] = \sqrt{N} \boldsymbol{F}_{N \times L} \boldsymbol{h}[m] \tag{41}$$

where $[\boldsymbol{F}_N]_{i, \ell} = e^{-j2\pi i \ell / N}$.

The receiver removes the cyclic prefix and performs a DFT. The received signal vector after these two operations is given by

$$\boldsymbol{y}[m] = \mathrm{diag}(\boldsymbol{g}[m])(\boldsymbol{S}\boldsymbol{b}[m] + \boldsymbol{p}[m]) + \boldsymbol{z}[m] \tag{42}$$

where complex additive white Gaussian noise with zero mean and covariance $\sigma_z^2 \boldsymbol{I}_N$ is denoted by $\boldsymbol{z}[m] \in \mathbb{C}^N$ with elements $z[m, q]$.

B. Multiuser Detector

The linear MMSE receiver detects the data using the received vector $\boldsymbol{y}[m]$, the spreading matrix $\boldsymbol{S}$, and the time-variant frequency response $\boldsymbol{g}[m]$, which is assumed to be known for the moment [18]. We define the time-variant effective spreading sequences

$$\tilde{\boldsymbol{s}}_k[m] = \mathrm{diag}(\boldsymbol{g}[m])\boldsymbol{s}_k \tag{43}$$

and the time-variant effective spreading matrix $\tilde{\boldsymbol{S}}[m] = [\tilde{\boldsymbol{s}}_1[m], \dots, \tilde{\boldsymbol{s}}_K[m]] \in \mathbb{C}^{N \times K}$ to express the unbiased time-variant linear MMSE filter

$$\boldsymbol{f}_k^H[m] = \frac{\tilde{\boldsymbol{s}}_k^H[m] \left(\sigma_z^2 \boldsymbol{I}_N + \tilde{\boldsymbol{S}}[m] \tilde{\boldsymbol{S}}^H[m] \right)^{-1}}{\tilde{\boldsymbol{s}}_k^H[m] \left(\sigma_z^2 \boldsymbol{I} + \tilde{\boldsymbol{S}}[m] \tilde{\boldsymbol{S}}^H[m] \right)^{-1} \tilde{\boldsymbol{s}}_k[m]}. \tag{44}$$

The code symbol estimates are given by $w_k[m] = \boldsymbol{f}_k^H[m] \boldsymbol{y}[m]$. After demapping and deinterleaving, the code bit estimates are supplied to the decoder. After the decoder, a hard decision is performed to obtain the transmitted data bits $\hat{\chi}_k[m'']$.

C. Slepian Basis Expansion Channel Estimator

The performance of the receiver crucially depends on the channel estimates for the time-variant frequency response $\boldsymbol{g}[m]$. The MC-CDMA signal model describes a transmission that takes place over N parallel frequency-flat channels. In order to reflect this, we rewrite (42) as a set of equations for every subcarrier $q \in \{0, \dots, N-1\}$,

$$y[m, q] = g[m, q]d[m, q] + z[m, q] \tag{45}$$

where $d[m, q]$ are the elements of $\boldsymbol{d}[m]$ [see (34)]. Comparing (45) with (2), we see that the structure of these equations are identical. The bandlimited property of $h[m, n]$ directly applies to $g[m, q]$ as well. This allows us to estimate the time-variant frequency-flat subcarrier $g[m, q]$ with the Slepian basis expansion (18). We define

$$\hat{\boldsymbol{\psi}}[q] = \left(\sum_{m \in \mathcal{P}} \boldsymbol{f}[m] \boldsymbol{f}^H[m] |p[m, q]|^2 \right)^{-1} \\ \cdot \sum_{m \in \mathcal{P}} y[m, q] p^*[m, q] \boldsymbol{f}^*[m] \tag{46}$$

where $q \in \{0, \dots, N-1\}$, and

$$\hat{\boldsymbol{\psi}}[q] = [\hat{\psi}_0[q], \dots, \hat{\psi}_{(D-1)}[q]]^T. \tag{47}$$

Although we will use the Slepian basis expansion, we keep the notation regarding the basis expansion generic. Hence, any basis expansion can be used for performance comparisons.

The estimated time-variant frequency response is given by $\hat{g}'[m, q] = \sum_{i=0}^{D-1} u_i[m] \hat{\psi}_i[q]$. Further noise suppression is obtained if we exploit the correlation between the subcarriers

$\hat{\boldsymbol{g}}[m] = \boldsymbol{F}_{N \times L} \boldsymbol{F}_{N \times L}^H \hat{\boldsymbol{g}}'[m]$. Finally, the channel estimates $\hat{\boldsymbol{g}}[m]$ are inserted into (43), and multiuser detection can be performed.

D. Simulation Results

The realizations of the time-variant frequency-selective channel $h'[n, \ell]$, sampled at the chip-rate $1/T_C$, are generated using an exponentially decaying power-delay profile $\eta^2[l]$ according to COST 259 [27]

$$\eta^2[\ell] = \frac{e^{-(\ell/4)}}{\sum_{\ell'=0}^{L-1} e^{-(\ell'/4)}} \quad (48)$$

for $\ell \in \{0, \ldots, L-1\}$. The discrete time indices n and ℓ denote sampling at rate $1/T_C = 3.84 \cdot 10^6 \text{ s}^{-1}$, as in the Universal Mobile Telecommunications System (UMTS). The root mean square delay spread of the power-delay profile in (48) is $T_D = 4T_C = 1 \mu\text{s}$, and its essential support $L = 15$. The autocorrelation for every channel tap is given by

$$R_{h'h'}[\tilde{n}, \ell] = \eta^2[\ell] J_0(2\pi\nu_D P\tilde{n}) \quad (49)$$

which results in the classical Jakes' spectrum. Each OFDM symbol has a length of P chips. We use the simulation model (52) for every channel tap $l \in \{0, \ldots, L-1\}$. The simulation uses a chip-rate sampled time-variant channel; thus, any possible effect from residual ICI would be visible in the simulation results.

The system operates at carrier frequency $f_C = 2 \text{ GHz}$, and the users move with velocity $v = 19.4 \text{ m/s}$. This gives $B_D = 126 \text{ Hz}$ and $\nu_D = 0.0026$. The number of subcarriers $N = 64$, and the OFDM symbol with cyclic prefix has length of $P = G + N = 79$. The block length $M = 256$. The system is designed for $v_{\max} = 28.5 \text{ m/s}$, which results in $D' = 3$. The Fourier basis expansion and the Slepian basis expansion, both applied for performance comparison, use the same dimensionality $D^{(F)} = D^{(S)} = 5$. We evaluate the performance of the Slepian basis expansion channel estimation with the lowest number of pilots possible $J = 5 = D$. Thus, we have as many pilots as basis functions in the basis expansion. The pilot ratio is 2%.

For data transmission, a convolutional, nonsystematic, nonrecursive, four-state, rate $R_C = 1/2$ code with generator polynomial $(5, 7)_8$ is used. The illustrated results are obtained by averaging over 400 independent channel realizations. The QPSK symbol energy is normalized to 1, and the E_b/N_0 is defined as

$$\frac{E_b}{N_0} = \frac{1}{2R_C\sigma_z^2} \frac{P}{N} \frac{M}{M-J}. \quad (50)$$

Fig. 10 illustrates the downlink MC-CDMA receiver performance with $K \in \{32, 64\}$ users in terms of BER versus E_b/N_0. Additionally, the plot also shows the single user bound, which is defined as the performance for one user $K = 1$ and a perfectly known channel $\boldsymbol{g}[m]$.

In order to relate the E_b/N_0 values in Fig. 10 to the channel estimation performance results in Section III, we establish the relation

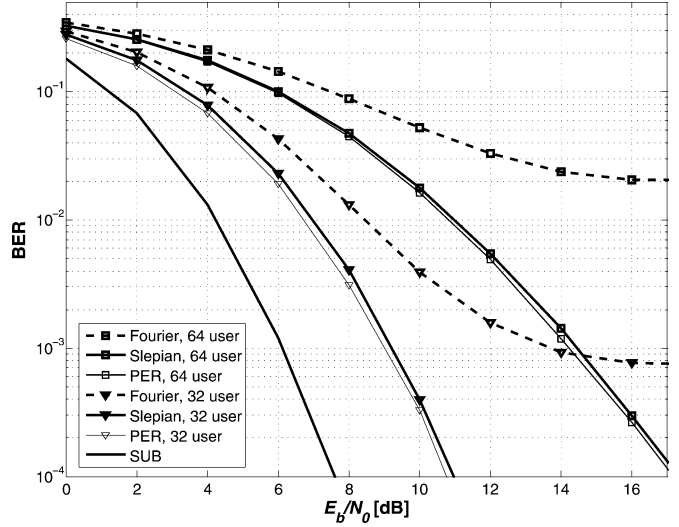$$\frac{E_S}{N_0} = \frac{K^2}{P} \frac{M-J}{M} \frac{E_b}{N_0} \quad (51)$$

Fig. 10. Downlink MC-CDMA receiver performance in terms of BER versus E_b/N_0. We compare the Slepian basis expansion and the Fourier basis expansion, all using $D = 5$ basis functions. The $K \in \{32, 64\}$ users are moving with $v = 19.4$ m/s, and the lowest amount of pilots possible $J = D = 5$ is used. For reference the single-user bound (SUB) and the performance with perfect channel knowledge (PER) are shown as well.

where we took the higher pilot energy in the downlink into account. For the simulation results with $K = 32$ users, the E_S/N_0 values for the simulation in Fig. 10 are in the range $11 \text{ dB} \leq E_S/N_0 \leq 28 \text{ dB}$. For $K = 64$ users, the range is from $17 \text{ dB} \leq E_S/N_0 \leq 34 \text{ dB}$.

Taking (51) into account when referring to Fig. 8 makes clear that the drastic reduced MSE_M for the Slepian basis expansion channel estimation leads to pronounced reduction in bit error rates if compared with the Fourier basis expansion. This is because the Fourier basis expansion is biased, as is visible for higher E_S/N_0 values in Fig. 8, which leads to an error floor in Fig. 10.

We also plot the receiver performance for a perfectly known channel (denoted "PER") in Fig. 10. The receiver performance is extremely close to the one with perfect channel knowledge when only as few as 2% pilots are used.

It is important to point out that we use a simulation model for the time-variant frequency-selective channel (see the Appendix) that is completely different from the basis expansion model, which we use for equalization. Thus, we proved the robustness of the Slepian basis expansion for a very realistic class of time-variant channels. Our results are therefore more general than the one presented in [11], which are limited to the class of Fourier basis expansion channels only.

VII. CONCLUSION

We showed that the Slepian basis expansion is very suitable to the modeling of a time-variant frequency-selective channel for the duration of a data block. The Slepian basis expansion is specified according to just two system parameters: the maximum Doppler bandwidth ν_{Dmax} and the block length M. A lower bound for the model order D results naturally.

We have compared the Fourier and the Slepian basis expansion for the same numerical complexity (same number of unknowns). The square bias of the Slepian basis expansion

compared with the Fourier basis expansion is three magnitudes smaller. We showed that the Slepian basis expansion outperforms the polynomial approach in [20] for normalized Doppler spreads $0.0023 < \nu_D$.

We presented simulation results for a fully loaded $K = N = 64$ MC-CDMA downlink for users moving at 19.4 m/s using a classic linear MMSE multiuser detector. The pilot ratio for channel estimation was 2% only. Applying the Slepian basis expansion for channel estimation, we achieved the same bit error rate performance as with perfect channel knowledge.

APPENDIX
SIMULATION MODEL FOR TIME-VARIANT CHANNELS WITH JAKES' SPECTRUM

We use the model from [28] with a correction for low velocities [29]. Our model ensures a Rayleigh distribution of $h[m]$ for all velocities v and even at $v = 0$ m/s. The detailed simulation model for $h[m]$ is defined as follows:

$$h[m] = \frac{1}{\sqrt{2}}(h_c[m] + jh_s[m]) \tag{52}$$

$$h_c[m] = \frac{2}{\sqrt{A}} \sum_{i=1}^{A} \cos(\psi_i) \cdot \cos(2\pi\nu_D m \cos\alpha_i + \phi_i)$$

$$h_s[m] = \frac{2}{\sqrt{A}} \sum_{i=1}^{A} \sin(\psi_i) \cdot \cos(2\pi\nu_D m \cos\alpha_i + \phi_i) \tag{53}$$

with

$$\alpha_i = \frac{2\pi i - \pi + \phi}{4A} \text{ for } i \in \{1, \ldots, A\}$$

where ϕ, ϕ_i, and ψ_i are independent and uniformly distributed over $[-\pi, \pi)$ for all i. For the numerical simulations, we fix the number of interfering paths to $A = 20$.

In the limit $\nu_D = 0$, (53) reduces to

$$h_c[m] = \frac{2}{\sqrt{A}} \sum_{i=1}^{A} \cos(\psi_i) \cdot \cos(\phi_i). \tag{54}$$

Because of the central limit theorem and the independence of all ψ_i and ϕ_i, the channel coefficients $h_c[m]$ are normally distributed. Therefore, the model converges to a block fading channel.

In [28], ϕ_i is replaced by the common phase ϕ. In this case, the distribution of the channel coefficients $h_c[m]$ is significantly different from a normal distribution.

ACKNOWLEDGMENT

REFERENCES

[1] C. Komninakis, C. Fragouli, A. H. Sayed, and R. D. Wesel, "Multi-input multi-output fading channel tracking and equalization using Kalman estimation," *IEEE Trans. Signal Process.*, vol. 50, no. 5, pp. 1065–1076, May 2002.

[2] M. Siala, "Maximum a posteriori semi-blind channel estimation for OFDM systems operating on highly frequency selective channels," *Ann. Telecommun.*, vol. 57, no. 9/10, pp. 873–924, Sep./Oct. 2002.

[3] T. Rappaport, *Wireless Communications—Principles & Practice*. Upper Saddle River, NJ: Prentice-Hall, 1996.

[4] M. Niedzwiecki, *Identification of Time-Varying Processes*. New York: Wiley, 2000.

[5] X. Zhao, J. Kivinen, P. Vainikainen, and K. Skog, "Characterization of Doppler spectra for mobile communications at 5.3 GHz," *IEEE Trans. Veh. Technol.*, vol. 52, no. 1, pp. 14–23, Jan. 2003.

[6] D. Schafhuber, G. Matz, and F. Hlawatsch, "Adaptive Wiener filters for time-varying channel estimation in wireless OFDM systems," in *Proc. IEEE Int. Conf. Acoust., Speech, Signal Process.*, vol. 4, Apr. 2003, pp. 688–691.

[7] P. Hoeher, "A statistical discrete-time model for the WSSUS multipath channel," *IEEE Trans. Veh. Technol.*, vol. 41, no. 4, pp. 461–468, Nov. 1992.

[8] G. B. Giannakis and C. Tepedelenlioglu, "Basis expansion models and diversity techniques for blind identification and equalization of time-varying channels," *Proc. IEEE*, vol. 96, no. 10, pp. 1969–1986, Oct. 1998.

[9] M. K. Tsatsanis and G. B. Giannakis, "Modeling and equalization of rapidly fading channels," *Int. J. Adaptive Control Signal Process.*, vol. 10, no. 2/3, pp. 159–176, Mar. 1996.

[10] A. M. Sayeed, A. Sendonaris, and B. Aazhang, "Multiuser detection in fast-fading multipath environment," *IEEE J. Sel. Areas Commun.*, vol. 16, no. 12, pp. 1691–1701, Dec. 1998.

[11] G. Leus, S. Zhou, and G. B. Giannakis, "Orthogonal multiple access over time- and frequency-selective channels," *IEEE Trans. Inf. Theory*, vol. 49, no. 4, pp. 1942–1950, Aug. 2003.

[12] J. G. Proakis and D. G. Manolakis, *Digital Signal Processing*, Third ed. Englewood Cliffs, NJ: Prentice-Hall, 1996.

[13] I. Barhumi, G. Leus, and M. Moonen, "Time-varying FIR equalization of doubly-selective channels," in *Proc. IEEE Int. Conf. Commun.*, vol. 5, Anchorage, AK, May 2003, pp. 3246–3250.

[14] T. Zemen, C. F. Mecklenbräuker, and R. R. Müller, "Time variant channel equalization for MC-CDMA via fourier basis functions," in *Proc. Multi-Carrier Spread-Spectrum Workshop*, Oberpfaffenhofen, Germany, Sep. 2003, pp. 451–454.

[15] D. Slepian, "Prolate spheroidal wave functions, Fourier analysis, and uncertainty—V: The discrete case," *Bell Syst. Tech. J.*, vol. 57, no. 5, pp. 1371–1430, May-Jun. 1978.

[16] T. Zemen and C. F. Mecklenbräuker, "Time-variant channel equalization via discrete prolate spheroidal sequences," in *Proc. 37th Asilomar Conf. Signals, Syst. Comput.*, Pacific Grove, CA, Nov. 2003, invited paper, pp. 1288–1292.

[17] W. Jakes, *Microwave Mobile Communications*. New York: Wiley, 1974.

[18] S. Verdú, *Multiuser Detection*. New York: Cambridge Univ. Press, 1998.

[19] H. J. Landau and H. O. Pollak, "Prolate spheroidal wave functions, Fourier analysis, and uncertainty—III: The dimension of the space of essentially time- and band-limited signals," *Bell Syst. Tech. J.*, vol. 41, no. 4, pp. 1295–1336, Jul. 1962.

[20] D. K. Borah and B. D. Hart, "Frequency-selective fading channel estimation with a polynomial time-varying channel model," *IEEE Trans. Commun.*, vol. 47, no. 6, pp. 862–873, Jun. 1999.

[21] X. Ma and G. B. Giannakis, "Maximum-diversity transmission over doubly selective wireless channels," *IEEE Trans. Inf. Theory*, vol. 49, no. 3, pp. 1832–1840, Jul. 2003.

[22] G. Leus, I. Barhumi, and M. Moonen, "Low-complexity serial equalization of doubly-selective channels," in *Proc. Baiona Workshop Signal Process. Commun.*, Baiona, Spain, Sep. 2003, pp. 60–74.

[23] Y. V. Zakharov, T. C. Tozer, and J. F. Adlard, "Polynomial spline-approximation of Clarke's model," *IEEE Trans. Signal Process.*, vol. 52, no. 5, pp. 1198–1208, May 2004.

[24] Z. Wang and G. B. Giannakis, "Wireless multicarrier communications," *IEEE Signal Process. Mag.*, vol. 17, no. 3, pp. 29–48, May 2000.

[25] Y. G. Li and L. J. Cimini, "Bounds on the interchannel interference of OFDM in time-varying impairments," *IEEE Trans. Commun.*, vol. 49, no. 3, pp. 401–404, Mar. 2001.

[26] G. Matz and F. Hlawatsch, "Time-frequency transfer function calculus (symbolic calculus) of linear time-varying systems (linear operators) based on generalized underspread theory," *J. Math. Phys.*, vol. 39, pp. 4041–4071, Aug. 1998.

[27] L. M. Correia, *Wireless Flexible Personalised Communications*. New York: Wiley, 2001.

[28] Y. R. Zheng and C. Xiao, "Simulation models with correct statistical properties for Rayleigh fading channels," *IEEE Trans. Commun.*, vol. 51, no. 6, pp. 920–928, Jun. 2003.

[29] T. Zemen and C. F. Mecklenbräuker, "Doppler diversity in MC-CDMA using the Slepian basis expansion model," in *Proc. 12th Eur. Signal Process. Conf.*, Vienna, Austria, Sep. 2004.

Thomas Zemen (S'03–M'05) was born in Mödling, Austria, in 1970. He received the Dipl.-Ing. and the Dr.techn. degrees (both with distinction) in 1998 and 2004, respectively, from Vienna University of Technology, Vienna, Austria, both in electrical engineering. He joined Siemens Austria, Vienna, in 1998, where he was hardware engineer and project manager for the radio communication devices department. From October 2001 to September 2003, he was delegated by Siemens Austria as a researcher to the mobile communications group at the Telecommunications Research Center Vienna (ftw.). Since October 2003, he has been with the Telecommunications Research Center Vienna, working as Researcher in the strategic I0 project. Since 2005, he has lead the "Future Mobile Communications Systems—Mathematical Modeling Analysis and Algorithms for Multi Antenna Systems" project, which was funded by the Vienna Science and Technology fund (WWTF). Currently, he teaches MIMO communications at the Vienna University of Technology. He has authored approximately 18 papers in international journals and conferences, for which he has also served as a reviewer. His research interests include orthogonal frequency division multiplexing (OFDM), multiuser detection, time-variant channel estimation, iterative receiver structures, and software defined radio concepts.

Christoph F. Mecklenbräuker (S'88–M'97) was born in Darmstadt, Germany, in 1967. He received the Dipl-Ing. degree in electrical engineering from Vienna University of Technology, Vienna, Austria, in 1992 and the Dr.-Ing. degree from Ruhr-University, Bochum, Germany, in 1998, both with distinction.

He worked for Siemens, Vienna, from 1997 to 2000, where he participated in the European framework of ACTS 90 "Future Radio Wideband Multiple Access System (FRAMES)." He was a delegate to the Third Generation Partnership Project (3GPP) and engaged in the standardization of the radio access network for UMTS. Since 2000, he has held a senior research position at the Telecommunications Research Center, Vienna (ftw.), in the field of mobile communications. Currently, he teaches 3G Mobile Networks at the Vienna University of Technology. He has authored around 60 papers in international journals and conferences, for which he has also served as a reviewer and holds eight patents in the field of mobile cellular networks. His current research interests include antenna array- and MIMO-signal processing for mobile communications, and ultra-wideband radio.

Dr. Mecklenbräuker is a member of the IEEE Signal Processing and Antennas and Propagation societies and EURASIP. His doctoral thesis on matched field processing received the Gert–Massenberg Prize in 1998.